Published in final edited form as:
J Biomech. 2009 March 11; 42(4): 517–523. doi:10.1016/j.jbiomech.2008.11.023.

Effects of suppression of bone turnover on cortical and trabecular load sharing in the canine vertebral body

Senthil K. Eswaran[a,*], **Grant Bevill**[a], **Prem Nagarathnam**[a], **Matthew R. Allen**[b], **David B. Burr**[b,c], and **Tony M. Keaveny**[a,d,1]

Senthil K. Eswaran: senthilk@me.berkeley.edu; Grant Bevill: gbevill@me.berkeley.edu; Prem Nagarathnam: theprem@berkeley.edu; Matthew R. Allen: matallen@iupui.edu; David B. Burr: dburr@iupui.edu; Tony M. Keaveny: tmk@me.berkeley.edu

[a] Orthopaedic Biomechanics Laboratory, Department of Mechanical Engineering, University of California, Berkeley, CA 94720, USA

[b] Department of Anatomy and Cell Biology, Indiana University School of Medicine, Indianapolis, IN 46202, USA

[c] Department of Orthopaedics, Indiana University, Indianapolis, IN 46202, USA

[d] Department of Bioengineering, University of California, Berkeley, CA 94720, USA

Abstract

The relative biomechanical effects of antiresorptive treatment on cortical thickness vs. trabecular bone microarchitecture in the spine are not well understood. To address this, T-10 vertebral bodies were analyzed from skeletally mature female beagle dogs that had been treated with oral saline (n = 8 control) or a high dose of oral risedronate (0.5 mg/kg/day, n = 9 RIS-suppressed) for 1 year. Two linearly elastic finite element models (36-μm voxel size) were generated for each vertebral body—a whole-vertebra model and a trabecular-compartment model—and subjected to uniform compressive loading. Tissue-level material properties were kept constant to isolate the effects of changes in microstructure alone. Suppression of bone turnover resulted in increased stiffness of the whole vertebra (20.9%, p = 0.02) and the trabecular compartment (26.0%, p = 0.01), while the computed stiffness of the cortical shell (difference between whole-vertebra and trabecular-compartment stiffnesses, 11.7%, p = 0.15) was statistically unaltered. Regression analyses indicated subtle but significant changes in the relative structural roles of the cortical shell and the trabecular compartment. Despite higher average cortical shell thickness in RIS-suppressed vertebrae (23.1%, p = 0.002), the maximum load taken by the shell for a given value of shell mass fraction was lower (p = 0.005) for the RIS-suppressed group. Taken together, our results suggest that—in this canine

[*]Corresponding author at. 23445 N 19th Avenue, Phoenix, AZ 85029 USA., Tel.: +1623 5874142; fax: +1623 5818814.
[1]Tel.: +1510 643 8017; fax: +1510 642 6163.

Conflicts of interest

Dr. Keaveny has served as a consultant/speaker for Merck & Co., Eli Lilly & Co., Novartis, GlaxoSmithKline, Amgen and Pfizer. He holds equity interests in O.N. Diagnostics, LLC, and has research grants from Merck & Co., Procter & Gamble Pharmaceuticals, and Pfizer. Dr. Burr and Dr. Allen have research grants from Eli Lilly & Co., Procter & Gamble/the Alliance for Better Bone Health and Amgen. Dr. Burr has served as a consultant to Procter & Gamble, Eli Lilly & Co. and Amgen, and has been supported as a speaker by Procter & Gamble, Eli Lilly & Co., Roche, and GlaxoSmithKlein. He also has a Material Transfer Agreement with Merck & Co.

model—the overall changes in the compressive stiffness of the vertebral body due to suppression of bone turnover were attributable more to the changes in the trabecular compartment than in the cortical shell. Such biomechanical studies provide an unique insight into higher-scale effects such as the biomechanical responses of the whole vertebra.

Keywords

Trabecular bone; Cortical shell; Suppressed bone turnover; Antiresorptive treatment; Microarchitecture; Bone quality; Load sharing

1. Introduction

Antiresorptive therapies have achieved substantial reductions in fracture risk that are not fully explained by changes in areal bone mineral density (Black et al., 2003; Cummings et al., 2002; Delmas, 2000). Potential differences in therapeutic effects of suppressed bone turnover on cortical vs. trabecular bone may be an important protective mechanism independent of changes in bone density, particularly for the spine given the thin nature but structural importance of the vertebral cortex (Eswaran et al., 2006a, b; Homminga et al., 2001). The effect of bisphosphonates on cortical shell thickness vs. trabecular bone microarchitecture and the associated changes in the biomechanics of the cortical vs. trabecular compartments in the spine is, therefore, of high clinical relevance.

In humans, in-vivo micro-CT and micro-MRI at peripheral sites can provide microstructural information—at resolutions close to the thickness of individual trabeculae—on treatment-induced changes in trabecular architecture and cortical thickness (Boutroy et al., 2005; Pistoia et al., 2003; van Rietbergen et al., 2002), while iliac crest biopsies can provide microstructure information at higher resolution (Borah et al., 2004; Chen et al., 2007). However, architectural effects of bisphosphonates at the iliac crest are difficult to extrapolate to the vertebra, particularly since trabecular architecture is so heterogeneous between these two sites (Amling et al., 1996; Chen et al., 2007; Eckstein et al., 2007). High-resolution clinical CT has been used to measure treatment effects on trabecular microarchitecture at the spine, but the resolution is relatively coarse and cortical thickness or biomechanical measurements have not yet been reported (Graeff et al., 2007). Regular clinical CT has been used in combination with finite element modeling to address treatment effects on cortical and trabecular compartments at the spine by computing the effects of removal of peripheral bone in the vertebral body (Keaveny et al., 2007).

As a result of these various limitations in the human studies, important insight on treatment effects can be gained from animal studies. Micro-CT, with and without finite element modeling, has been used in rat (Ito et al., 2002), monkey (Fox et al., 2007; Muller et al., 2004), and canine studies (Day et al., 2004; Ding et al., 2003; Eswaran et al., 2007) to investigate treatment effects on trabecular microarchitecture and whole-bone strength but not on cortical thickness. Using a canine model, Allen et al. (Allen et al., 2006c; Allen and Burr, 2008) found no significant change in the whole-vertebral strength per unit areal BMD (measured by DXA) due to bisphosphonate treatment—suggesting that increased mechanical strength was due entirely to increased density without changes in bone quality (Hernandez and Keaveny, 2006)—but did not parse out the individual contributions of the trabecular bone and cortical shell. Thus, at this juncture, there is uncertainty regarding the effect of bisphosphonates on cortical shell thickness vs. trabecular bone microarchitecture, and how this affects the relative biomechanical properties of the vertebral trabecular vs. cortical compartments.

Our overall goal was to address this issue using a large animal model. We performed high-resolution micro-CT scans and finite element modeling of vertebrae excised from dogs that had been treated with high doses of risedronate or vehicle. Our specific objectives were to determine the effect of turnover suppression on (1) cortical thickness, trabecular microarchitecture, and the relative masses of these two compartments; and (2) the relative load sharing between the trabecular and cortical bone. This study is unique because it is the first to investigate the biomechanical effects of microstructural changes induced by suppressed bone turnover with particular emphasis on cortical vs. trabecular load sharing.

2. Methods

Details of the experimental design have been published previously (Allen et al., 2006b). Briefly, female beagle dogs, aged 1–2 years, were given oral saline (control group, $n = 10$) or a high dose (0.5 mg/kg/day) of oral risedronate (RIS-suppressed group, $n = 10$) daily for a period of 1 year. This dosage of risedronate is five-fold higher than the clinical dose used to treat post-menopausal osteoporosis (equivalent to the dose used to treat Paget's disease) and was chosen to maximize suppression of bone turnover. Turnover suppression in the vertebra was significantly greater with this higher dose of risedronate compared to the dose equivalent to that used for treatment of post-menopausal osteoporosis (Allen et al., 2006b). After retrieval, the T-10 vertebral bodies were scanned at 18 μm voxel size using micro-CT (Scanco 80, Basserdorf, Switzerland), thresholded using a global threshold value chosen based on an adaptive threshold algorithm (provided as part of the scanner), and region-averaged to 36 μm voxel size. Two specimens from the control group and one from the RIS-suppressed group were eliminated from this study since they exhibited artifactual endplate damage.

An averaging technique (Eswaran et al., 2006a, b) was used within an image processing software (IDL, Research Systems Inc., Boulder, CO) to identify the cortical shell in the region excluding the endplates (Fig. 1). The average thickness of the anterior cortical shell (Ct.Th) was determined using custom code (Eswaran et al., 2006a, b), the anterior half being chosen for measurement in order to avoid any errors due to the presence of the basivertebral foramen. Two cylindrical cores (diameter = 3.5 mm, height = 6 mm nominal dimensions) were virtually removed from each scan such that the basivertebral foramen and the cortex were avoided (Eswaran et al., 2007). Trabecular microarchitecture data obtained from the two cores were averaged per vertebra. An average cross-sectional area of the vertebral body was calculated as the average of the cross-sectional areas of 1-mm-thick transverse slices located at 25% and 75% of the vertebral height.

The shell mass fraction was calculated as the shell mass divided by the total bone mass in the region excluding the endplates. The total bone mass was calculated as the total volume of bone elements multiplied by an assumed uniform tissue density of 2.05 g/cm^3 (Morgan et al., 2003) for all bone elements. While there is evidence that bisphosphonates increase the mineralization in trabecular bone (Allen et al., 2006b; Boivin et al., 2000; Burr et al., 2003; Roschger et al., 2001), we deliberately eliminated this effect in the models in order to evaluate the mechanical consequences of suppression-induced changes only within the microstructure. The same tissue-level elastic properties—a Young's modulus E of 18.5 GPa and a Poisson's ratio ν of 0.3 (Bevill et al., 2006)—were assigned to all specimens in both the control and RIS-suppressed groups in order to eliminate any treatment effects on tissue-level material properties, thereby providing tissue-normalized outcomes. A layer of PMMA ($E = 2500$ MPa, $\nu = 0.3$ (Lewis, 1997)) was added over the endplates of the vertebral body to provide uniform loading conditions across all vertebrae and to simulate commonly used laboratory test conditions (Crawford et al., 2003).

Using custom code with a parallel mesh partitioner and multigrid solver (Adams et al., 2004), two linear finite element analyses were performed for each vertebra—an intact whole-vertebra model, and a trabecular-compartment model consisting of the entire vertebra but with the cortical shell being virtually removed. Each model had approximately 40–110 million degrees of freedom and analyses were run on an IBM-SP4 supercomputer (Datastar, San Diego) using a maximum of 320 processors in parallel, requiring a total of approximately 1700 CPU hours.

From the architectural analysis, the relationship between average cortical shell thickness and mean trabecular thickness was determined. From the finite element analyses, the tissue-normalized stiffness of the whole vertebra and the trabecular compartment were computed. The stiffness of the cortical shell was computed as the difference between the whole-vertebra stiffness and trabecular-compartment stiffness. The shell load fraction (defined as the ratio of shell load to total load) was calculated for each transverse cross-section and plotted as a function of axial position for the intact model (Eswaran et al., 2006b). From this, the maximum values of load fraction for the cortical shell and trabecular bone over any transverse section were determined for each vertebral body (Fig. 1). The maximum trabecular load fraction equivalently represents the minimum cortical shell load fraction (trabecular load fraction = 1–shell load fraction). The relationship between maximum shell load fraction, maximum trabecular load fraction, and shell mass fraction was investigated. The relationships between the stiffness of the trabecular compartment, cortical shell, and the whole vertebra were also determined. The ratio of vertebral stiffness to bone mass and the correlation between vertebral stiffness and bone mass were determined.

An unpaired Student's *t*-test (JMP 5.0, SAS Institute Inc., Cary, NC) was performed to test treatment effects on the mean values of the outcome variables. The effect of suppressed bone turnover on the various relationships (vertebral stiffness and bone mass;trabecular-compartment, cortical shell, and whole vertebra stiffness; maximum shell load fraction, maximum trabecular load fraction, and shell mass fraction) was tested (slope and intercept) using a generalized linear regression model. A value of $p<0.05$ was considered significant.

3. Results

The anterior cortical shell thickness (Ct. Th) and mean trabecular bone thickness (Tb.Th) both significantly increased due to suppression of bone turnover, the effect being two-fold greater on a percentage basis for the cortical shell (23.1%) than for the trabecular bone (11.5%, Table 1). There was no significant correlation between average cortical shell thickness and mean trabecular thickness for either control or RIS-suppressed groups indicating that these thickness measures represented independent responses (Fig. 2). The effect of bone-turnover suppression on the relative amount of cortical vs. trabecular bone mass and the cross-sectional area of the vertebral body did not reach statistical significance (Table 1).

The mean values of the load sharing outcomes—maximum shell load fraction and maximum trabecular load fraction—were not significantly altered due to suppression of bone turnover (Table 2). However, the relationship between maximum shell load fraction and shell mass fraction ($p_{\text{intercept}} = 0.005$, $p_{\text{slope}} = 0.51$), was significantly altered by suppression of bone turnover (Fig. 3A) such that for a given shell mass fraction, the maximum shell load fraction of the treated group was lower than that of the control group. The maximum shell load fraction and maximum trabecular load fraction were significantly correlated for the treated group but not for the control group (Fig. 3B).

Virtual removal of the cortical shell revealed that the trabecular compartment accounted for about two-thirds of the whole-vertebra stiffness (Table 2). While the change in stiffnesses of the trabecular compartment and whole vertebra were statistically significant, the change in

cortical shell stiffness did not reach statistical significance (Table 2). There was a non-significant trend for the ratio of the trabecular-compartment stiffness to the whole-vertebra stiffness to increase (4.7%, $p = 0.11$) due to suppression of bone turnover. The regression between cortical shell stiffness and whole-vertebra stiffness was statistically significant for the RIS-suppressed group ($p = 0.002$), but not for the control group ($p = 0.53$, Fig. 4).

4. Discussion

Our overall goal was to determine the mechanical consequences of turnover suppression-induced changes in the cortical shell thickness and trabecular microarchitecture within the canine vertebral body. We deliberately isolated the effects of changes in microstructure by assigning all bone tissue in the two treatment groups the same tissue material characteristics, thereby providing complementary data to the existing experimental data on whole-vertebra treatment effects from the literature. The stiffness for the whole-vertebral body (20.9%, $p = 0.02$) and the trabecular compartment (26.0%, $p = 0.01$) increased significantly with suppression of bone turnover, while the change in computed stiffness of the cortical shell was not significant (11.7%, $p = 0.15$). Regression analysis indicated subtle but significant changes in the relative structural roles of the cortical shell and the trabecular compartment. For a given value of shell mass fraction, the maximum load taken by the shell was lower for the RIS-suppressed group as compared to the control group (Fig. 3). This effect was despite a mean increase in average cortical shell thickness of 23.1% due to suppression of bone turnover, indicating that local variations in cortical shell thickness and trabecular microarchitecture affect the biomechanical response and may not necessarily be captured by “global” metrics such as average cortical shell thickness. Taken together, our results suggest that the overall changes in the compressive stiffness of the canine vertebra were attributable more to the changes in the trabecular compartment than the cortical shell and highlight the importance of such biomechanical studies in order to evaluate the higher-scale biomechanical responses.

The main strength of this study was our use of previously established techniques to identify and measure the average thickness of the cortical shell (Eswaran et al., 2006a, b), and the use of high-resolution micro-CT-based finite element analysis on whole vertebrae. This allowed us to quantify the relative amount of cortical vs. trabecular bone mass as well as the relative load distribution between the cortical shell and trabecular bone. Homogeneous material properties were assigned to control and suppressed bone, thereby allowing us to isolate the mechanical consequences of suppressed bone turnover due only to changes in cortical shell thickness and trabecular microarchitecture. Another key aspect of this study was the insight made possible by our virtual removal of the cortical shell. This enabled us to extract subtle effects due to the treatment on the relative roles of the cortical shell and trabecular compartment that would otherwise have gone undetected. We also performed a detailed convergence study on a subset of specimens (data on file) that showed comparable results between models with 18 and 36 μm voxel size.

One limitation of this study was the use of a non-osteoporotic animal model, because the effect of suppressed bone turnover may depend on the baseline level of trabecular bone volume fraction, the microarchitecture of the trabecular bone, and the thickness of the cortical shell. Also, we did not address failure behavior since only linearly elastic finite element analyses were performed. The relatively high trabecular bone volume fraction (Table 1) of the control specimens would likely minimize any influence of failure mechanisms associated with large deformations, such as bending (Bevill et al., 2006) or buckling (Gibson, 1985) and thus, the strength trends may differ particularly in very low-density osteoporotic bone. Our analysis used uniform compressive loading via a PMMA layer in order to mimic controlled conditions commonly used in experimental testing of isolated vertebrae (Eriksson et al., 1989;Faulkner et al., 1991;Kopperdahl et al., 2000). Further research is required to study the effects of

treatment on the vertebral body under combined compression and anterior–posterior flexion, including the presence of the disc. These were not undertaken in this canine study, because any such effects are likely specific to the human vertebra given the difference in physiological loading between dogs and humans.

The risedronate dosage was five-times higher than the clinical dose for treatment of post-menopausal osteoporosis and equivalent to the dosage used for treatment of Paget's disease, though the dose regimen was different. As a result, care should be taken in interpreting the results of this study in a clinical context. This study was also limited in its statistical power to detect changes in the vertebral stiffness–bone mass relationship, due in parts to the relatively small sample size and the differences in the range of the explanatory variable (bone mass) for the control and suppressed groups. While this study focused on the effects of treatment-induced changes in the microstructure, there may be differential effects of treatment on the tissue-level material properties of cortical and trabecular bone. At this juncture, there are limited data available in the literature in this regard. If the tissue-level material properties of cortical and trabecular bone exhibit the same changes, then the results of this study remain unchanged. Since bisphosphonate treatment does not affect periosteal osteoblast activity (Allen et al., 2006a), it is possible that the trabecular tissue may become more mineralized than cortical tissue with treatment. In such a scenario, the effect of treatment on the stiffness of the trabecular compartment would increase (from the current 26.0%) and the trabecular compartment would be a greater contributor to the increased stiffness of the whole-vertebral body than the one reported in this study.

Comparison of the shell mass fraction and load-sharing outcomes from this study with previous data on elderly female human vertebrae (Eswaran et al., 2006b) (age = 75±9 years) indicated a similarity in the load-sharing characteristics (Fig. 5). However, the ratio of stiffness of the trabecular compartment to the stiffness of the whole vertebra for the canine model (0.64±0.05) was substantially higher than that for the human vertebra (0.48±0.09) (Eswaran et al., 2006a). This trend may be attributable to the differences in trabecular spacing between the canine (0.39 ±0.03 mm, Table 1) and human vertebra (0.80± 0.13 mm, (Ulrich et al., 1999)). Virtual removal of the cortical shell results in unloading of the peripheral trabeculae and leads to an underestimation of the contribution of the trabecular compartment to the whole-vertebral stiffness (Eswaran et al., 2006a), an effect which would be greater in models having larger trabecular spacing (Un et al., 2006).

Clinically, the cortical shell may be an important component in the etiology of spine fractures (Melton et al., 2007). In that context, this study—to the best of our knowledge—is the first to measure the effects of suppressed bone turnover on the cortical shell thickness in the canine vertebral body and quantify the relative structural roles of the cortical shell and trabecular bone. Previous analyses on trabecular bone cores from canine vertebra have found that strength increases due to suppression of bone turnover were entirely commensurate with increase in bone volume fraction (Eswaran et al., 2007; Allen and Burr, 2008) and that there was no net effect of treatment on the tissue-level elastic modulus (Day et al., 2004). Our results suggest that the overall effects of treatment on the vertebral body were dominated by changes in the trabecular compartment. These data are consistent with the previous results that bisphosphonates had no significant effect on periosteal osteoblast activity of the rib (Allen et al., 2006a) and hence, the treatment effects on the vertebral strength are largely due to their effect on remodeling-associated formation activities—such as those on endocortical and trabecular envelopes—rather than on modeling-associated formation activities—such as those on periosteal surfaces. Our results are—to some extent—consistent with a clinical study involving alendronate treatment in osteoporotic women (Keaveny et al., 2007) which found, using parametric studies, that the FE-measured (typical element size of 1 mm) increases in trabecular strength were comparable to those in whole-vertebral strength. In this study, we

found that treatment resulted in a 26.0% increase in trabecular stiffness as compared to a 20.9% increase in whole-vertebral stiffness. Differences in results may be due to the differences in canine vs. human physiology and vertebral structure, treatments, and/or, analysis techniques. In summary, our results suggest that, at least for the spine, the effect of high-dose risedronate treatment on canine whole-vertebra structural behavior is largely through changes in the trabecular compartment. Such biomechanical studies can provide unique insight into higher-scale effects such as the biomechanical responses of the whole vertebra.

Acknowledgments

Funding was provided via an unrestricted gift by Procter and Gamble Pharmaceuticals Inc., and research grants provided by the National Institute of Health (AR49828, AR47838) and the Alliance for Better Bone Health. This investigation utilized a facility constructed with support from Research Facilities Improvement Program Grant number C06 RR10601-01 from the National Center for Research Resources, National Institutes of Health. Computational resources were available through Grant UCB-266 from the National Partnership for Computational Infrastructure. All the finite element analyses were performed on an IBM Power4 supercomputer (Datastar, San Diego Supercomputer Center). We would like to thank Judd Day (Exponent Inc., Philadelphia) for micro-CT imaging the specimens. Dr. Keaveny has a financial interest in O.N. Diagnostics and both he and the company may benefit from the results of this research.

References

Adams, MF.; Bayraktar, HH.; Keaveny, TM.; Papadopoulos, P. Ultrascalable implicit finite element analyses in solid mechanics with over a half a billion degrees of freedom. Paper presented at ACM/IEEE Proceedings of SC2004: High Performance Networking and Computing; 2004.

Allen MR, Follet H, Khurana M, Sato M, Burr DB. Antiremodeling agents influence osteoblast activity differently in modeling and remodeling sites of canine rib. Calcif Tissue Int 2006a;79 (4):255–261. [PubMed: 17033724]

Allen MR, Iwata K, Phipps R, Burr DB. Alterations in canine vertebral bone turnover, microdamage accumulation, and biomechanical properties following 1-year treatment with clinical treatment doses of risedronate or alendronate. Bone 2006b;39 (4):872–879. [PubMed: 16765660]

Allen MR, Iwata K, Sato M, Burr DB. Raloxifene enhances vertebral mechanical properties independent of bone density. Bone 2006c;39 (5):1130–1135. [PubMed: 16814622]

Allen MR, Burr DB. Changes in vertebral strength-density and energy absorption-density relationships following bisphosphonate treatment in beagle dogs. Osteoporos Int 2008;19 (1):95–99. [PubMed: 17710353]

Amling M, Herden S, Posl M, Hahn M, Ritzel H, Delling G. Heterogeneity of the skeleton: comparison of the trabecular microarchitecture of the spine, the iliac crest, the femur, and the calcaneus. J Bone Miner Res 1996;11 (1):36–45. [PubMed: 8770695]

Bevill G, Eswaran SK, Gupta A, Papadopoulos P, Keaveny TM. Influence of bone volume fraction and architecture on computed large-deformation failure mechanisms in human trabecular bone. Bone 2006;39 (6):1218–1225. [PubMed: 16904959]

Black DM, Greenspan SL, Ensrud KE, Palermo L, McGowan JA, Lang TF, Garnero P, Bouxsein ML, Bilezikian JP, Rosen CJ. The effects of parathyroid hormone and alendronate alone or in combination in postmenopausal osteoporosis. N Engl J Med 2003;349 (13):1207–1215. [PubMed: 14500804]

Boivin GY, Chavassieux PM, Santora AC, Yates J, Meunier PJ. Alendronate increases bone strength by increasing the mean degree of mineralization of bone tissue in osteoporotic women. Bone 2000;27 (5):687–694. [PubMed: 11062357]

Borah B, Dufresne TE, Chmielewski PA, Johnson TD, Chines A, Manhart MD. Risedronate preserves bone architecture in postmenopausal women with osteoporosis as measured by three-dimensional microcomputed tomography. Bone 2004;34 (4):736–746. [PubMed: 15050906]

Boutroy S, Bouxsein ML, Munoz F, Delmas PD. In vivo assessment of trabecular bone microarchitecture by high-resolution peripheral quantitative computed tomography. J Clin Endocrinol Metab 2005;90 (12):6508–6515. [PubMed: 16189253]

Burr DB, Miller L, Grynpas M, Li J, Boyde A, Mashiba T, Hirano T, Johnston CC. Tissue mineralization is increased following 1-year treatment with high doses of bisphosphonates in dogs. Bone 2003;33 (6):960–969. [PubMed: 14678856]

Chen P, Miller PD, Recker R, Resch H, Rana A, Pavo I, Sipos AA. Increases in BMD correlate with improvements in bone microarchitecture with teriparatide treatment in postmenopausal women with osteoporosis. J Bone Miner Res 2007;22 (8):1173–1180. [PubMed: 17451369]

Crawford RP, Cann CE, Keaveny TM. Finite element models predict in vitro vertebral body compressive strength better than quantitative computed tomography. Bone 2003;33 (4):744–750. [PubMed: 14555280]

Cummings SR, Karpf DB, Harris F, Genant HK, Ensrud K, LaCroix AZ, Black DM. Improvement in spine bone density and reduction in risk of vertebral fractures during treatment with antiresorptive drugs. Am J Med 2002;112 (4):281–289. [PubMed: 11893367]

Day JS, Ding M, Bednarz P, van der Linden JC, Mashiba T, Hirano T, Johnston CC, Burr DB, Hvid I, Sumner DR, Weinans H. Bisphosphonate treatment affects trabecular bone apparent modulus through micro-architecture rather than matrix properties. J Orthop Res 2004;22 (3):465–471. [PubMed: 15099622]

Delmas PD. How does antiresorptive therapy decrease the risk of fracture in women with osteoporosis? Bone 2000;27 (1):1–3. [PubMed: 10865202]

Ding M, Day JS, Burr DB, Mashiba T, Hirano T, Weinans H, Sumner DR, Hvid I. Canine cancellous bone microarchitecture after one year of high-dose bisphosphonates. Calcif Tissue Int 2003;72 (6): 737–744. [PubMed: 14563003]

Eckstein F, Matsuura M, Kuhn V, Priemel M, Muller R, Link TM, Lochmuller EM. Sex differences of human trabecular bone microstructure in aging are site-dependent. J Bone Miner Res 2007;22 (6): 817–824. [PubMed: 17352643]

Eriksson SAV, Isberg BO, Lindgren JU. Prediction of vertebral strength by dual photon-absorptiometry and quantitative computed tomography. Calcif Tissue Int 1989;44 (4):243–250. [PubMed: 2501006]

Eswaran SK, Bayraktar HH, Adams MF, Gupta A, Hoffman PF, Lee DC, Papadopoulos P, Keaveny TM. The micro-mechanics of cortical shell removal in the human vertebral body. Comput Methods Appl Mech Eng 2006a;196 (31–32):3025–3032.

Eswaran SK, Gupta A, Adams MF, Keaveny TM. Cortical and trabecular load sharing in the human vertebral body. J Bone Miner Res 2006b;21 (2):307–314. [PubMed: 16418787]

Eswaran SK, Allen MR, Burr DB, Keaveny TM. A computational assessment of the independent contribution of changes in canine trabecular bone volume fraction and microarchitecture to increased bone strength with suppression of bone turnover. J Biomech 2007;40 (15):3424–3431. [PubMed: 17618634]

Faulkner KG, Cann CE, Hasegawa BH. Effect of bone distribution on vertebral strength: assessment with patient-specific nonlinear finite element analysis. Radiology 1991;179 (3):669–674. [PubMed: 2027972]

Fox J, Miller MA, Newman MK, Recker RR, Turner CH, Smith SY. Effects of daily treatment with parathyroid hormone 1–84 for 16 months on density, architecture and biomechanical properties of cortical bone in adult ovariectomized rhesus monkeys. Bone 2007;41 (3):321–330. [PubMed: 17573250]

Gibson LJ. The mechanical behavior of cancellous bone. J Biomech 1985;18 (5):317–328. [PubMed: 4008502]

Graeff C, Timm W, Nickelsen TN, Farrerons J, Marin F, Barker C, Gluer CC. Monitoring teriparatide-associated changes in vertebral microstructure by high-resolution CT in vivo: results from the EUROFORS study. J Bone Miner Res 2007;22 (9):1426–1433. [PubMed: 17547537]

Hernandez CJ, Keaveny TM. A biomechanical perspective on bone quality. Bone 2006;39 (6):1173–1181. [PubMed: 16876493]

Homminga J, Weinans H, Gowin W, Felsenberg D, Huiskes R. Osteoporosis changes the amount of vertebral trabecular bone at risk of fracture but not the vertebral load distribution. Spine 2001;26 (14):1555–1561. [PubMed: 11462085]

Ito M, Nishida A, Koga A, Ikeda S, Shiraishi A, Uetani M, Hayashi K, Nakamura T. Contribution of trabecular and cortical components to the mechanical properties of bone and their regulating parameters. Bone 2002;31 (3):351–358. [PubMed: 12231406]

Keaveny TM, Donley DW, Hoffmann PF, Mitlak BH, Glass EV, San Martin JA. Effects of teriparatide and alendronate on vertebral strength as assessed by finite element modeling of QCT scans in women with osteoporosis. J Bone Miner Res 2007;22 (1):149–157. [PubMed: 17042738]

Kopperdahl DL, Pearlman JL, Keaveny TM. Biomechanical consequences of an isolated overload on the human vertebral body. J Orthop Res 2000;18 (5):685–690. [PubMed: 11117287]

Lewis G. Properties of acrylic bone cement: state of the art review. J Biomed Mater Res 1997;38 (2): 155–182. [PubMed: 9178743]

Melton J, Riggs BL 3rd, Keaveny TM, Achenbach SJ, Hoffman PF, Camp JJ, Rouleau PA, Bouxsein ML, Amin S, Atkinson EJ, Robb RA, Khosla S. Structural determinants of vertebral fracture risk. J Bone Miner Res 2007;22 (12):1885–1892. [PubMed: 17680721]

Morgan EF, Bayraktar HH, Keaveny TM. Trabecular bone modulus–density relationships depend on anatomic site. J Biomech 2003;36 (7):897–904. [PubMed: 12757797]

Muller R, Hannan M, Smith SY, Bauss F. Intermittent ibandronate preserves bone quality and bone strength in the lumbar spine after 16 months of treatment in the ovariectomized cynomolgus monkey. J Bone Miner Res 2004;19 (11):1787–1796. [PubMed: 15476578]

Pistoia W, van Rietbergen B, Ruegsegger P. Mechanical consequences of different scenarios for simulated bone atrophy and recovery in the distal radius. Bone 2003;33 (6):937–945. [PubMed: 14678853]

Roschger P, Rinnerthaler S, Yates J, Rodan GA, Fratzl P, Klaushofer K. Alendronate increases degree and uniformity of mineralization in cancellous bone and decreases the porosity in cortical bone of osteoporotic women. Bone 2001;29 (2):185–191. [PubMed: 11502482]

Ulrich D, van Rietbergen B, Laib A, Ruegsegger P. The ability of three-dimensional structural indices to reflect mechanical aspects of trabecular bone. Bone 1999;25 (1):55–60. [PubMed: 10423022]

Un K, Bevill G, Keaveny TM. The effects of side-artifacts on the elastic modulus of trabecular bone. J Biomech 2006;39 (11):1955–1963. [PubMed: 16824533]

van Rietbergen B, Majumdar S, Newitt D, MacDonald B. High-resolution MRI and micro-FE for the evaluation of changes in bone mechanical properties during longitudinal clinical trials: application to calcaneal bone in postmenopausal women after one year of idoxifene treatment. Clin Biomech (Bristol, Avon) 2002;17 (2):81–88.

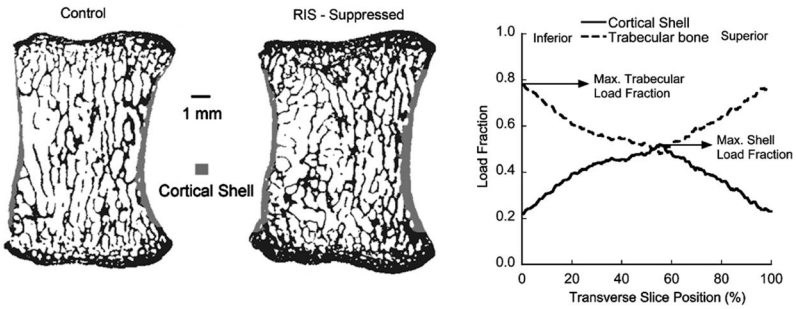

Fig. 1.

Left: Sagittal slice of a control- and RIS-suppressed vertebra with the cortical shell identified in the region excluding the endplates. *Right*: Typical variation of the load sharing between cortical shell and trabecular bone across transverse slices of the vertebral body in the region excluding the endplates.

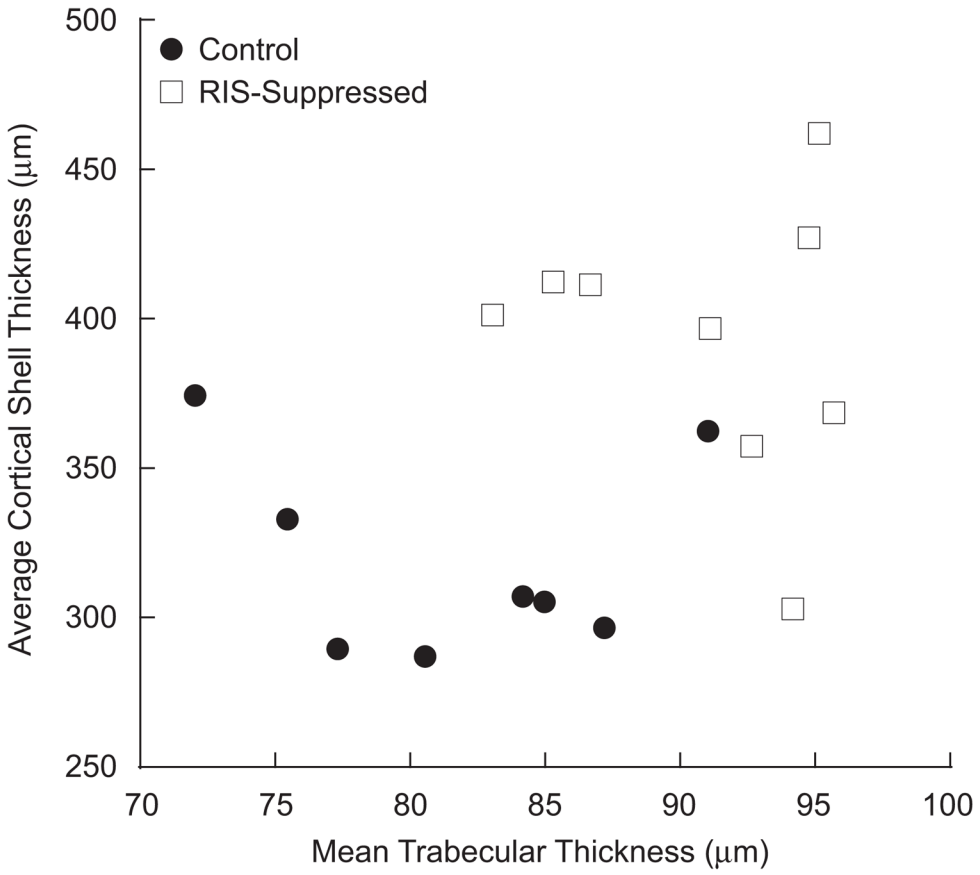

Fig. 2.
Variation of average cortical shell thickness vs. mean trabecular thickness showing no correlation between these variables for the control ($p = 0.70$) or RIS-suppressed ($p = 0.66$) groups. The mean values for both cortical and trabecular thickness were higher for the suppressed group ($p = 0.002$ and 0.004, respectively).

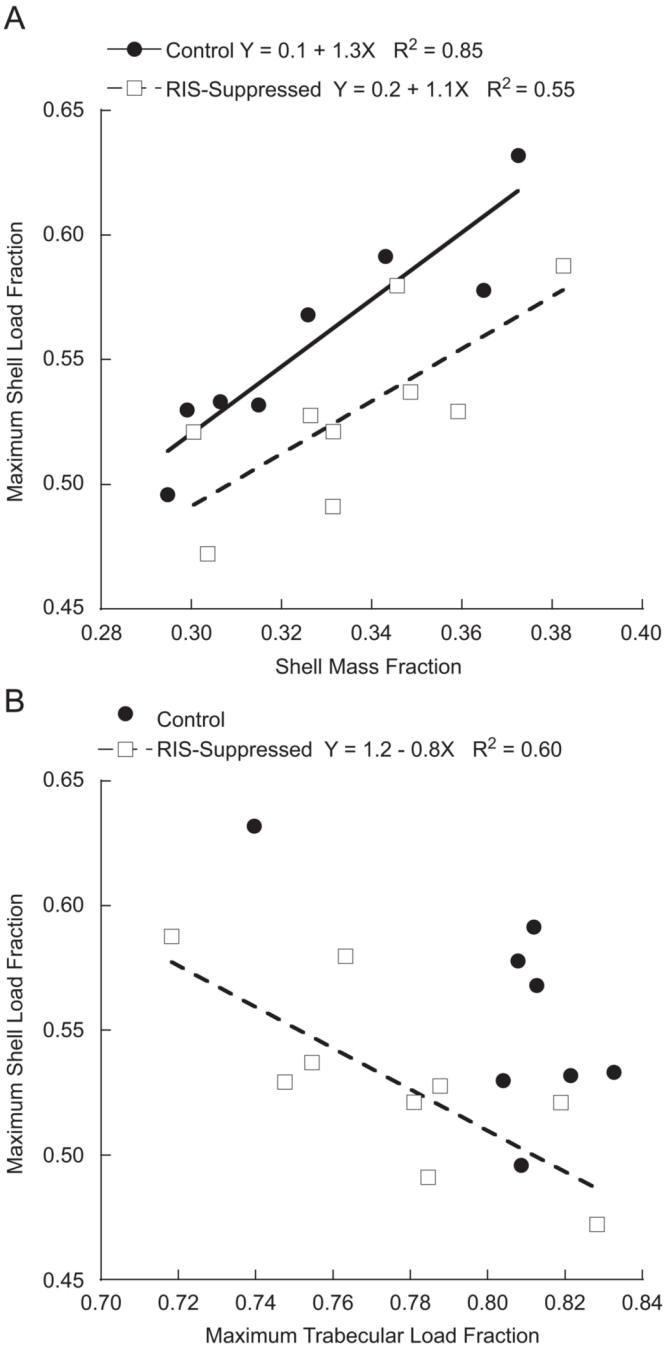

Fig. 3.

(A) Variation of maximum shell load fraction with shell mass fraction for the control and suppressed groups showing that there was a significant change in the intercept of the regression due to suppression of bone turnover ($p_{intercept} = 0.005$, $p_{slope} = 0.51$). (B) The regression between the maximum shell load fraction and maximum trabecular load fraction was statistically significant for the RIS-suppressed group ($p = 0.01$), but not for the control group ($p = 0.06$).

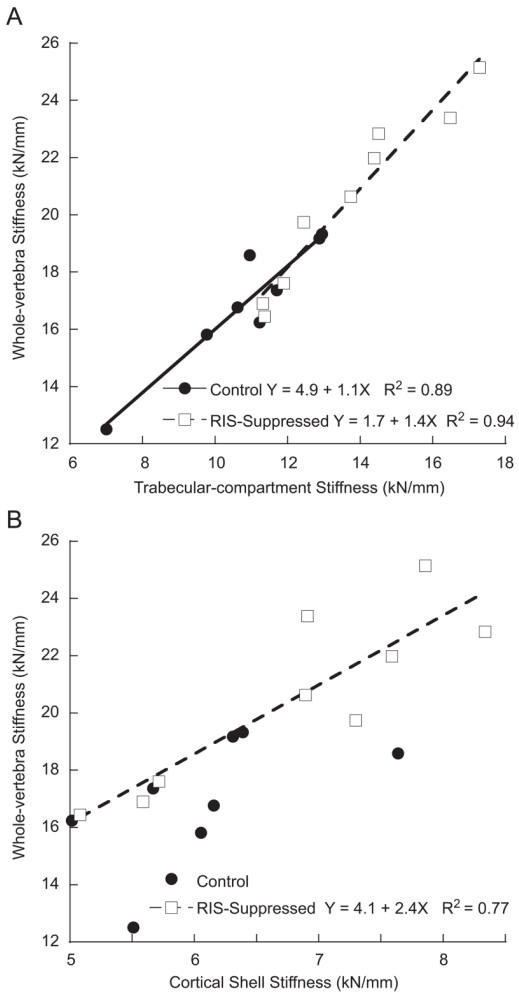

Fig. 4.

The relationship between whole-vertebra stiffness and trabecular-compartment stiffness (A) was not altered ($p_{intercept} = 0.91$, $p_{slope} = 0.22$) by suppression of bone turnover. The regression between whole-vertebra stiffness and cortical shell stiffness (B) was statistically significant for the RIS-supressed group ($p = 0.002$), but not for the control group ($p = 0.53$). Note that stiffness measures were computed assuming a constant tissue-level elastic modulus for control and suppressed groups.

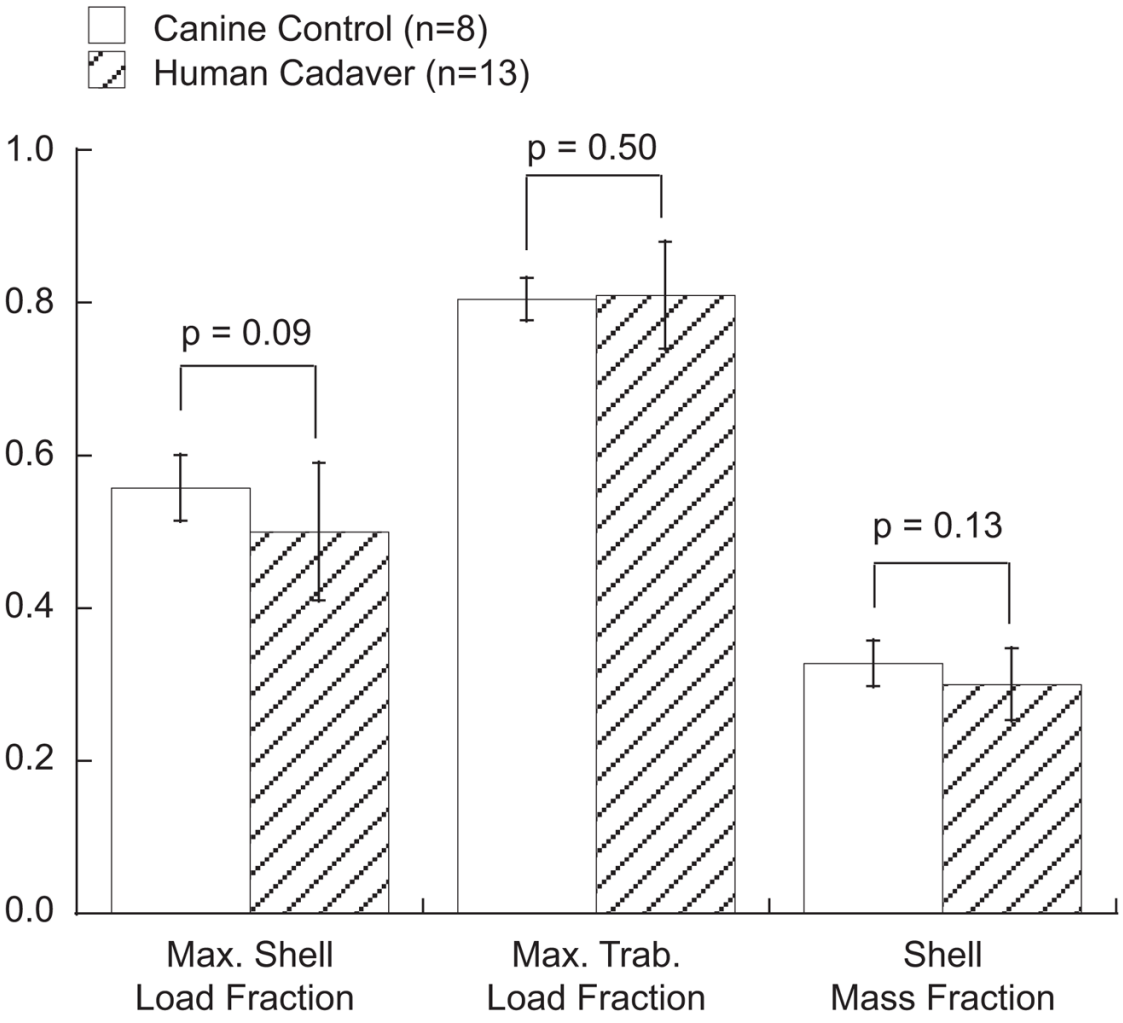

Fig. 5.

The mean values of the maximum load fraction taken by the shell and trabecular bone, and the shell mass fraction of the canine vertebral body were similar to those of elderly female human vertebrae (Eswaran et al., 2006b), supporting the use of the canine model for these outcomes.

Table 1

Comparison of the trabecular microarchitecture, average thickness of the cortical shell, and bone mass measurements made using micro-CT between the control- (n = 8) and RIS-suppressed (n = 9) groups.

	Control	RIS-suppressed	Percent[a]	p-Value[b]
Trabecular bone				
BV/TV	0.20±0.02	0.24±0.01	21.9	0.0002
Trabecular spacing (mm)	0.39±0.03	0.36±0.03	−8.1	0.03
Mean trabecular thickness (μm)	82±6	91±5	11.5	0.004
Average thickness of the cortical shell (μm)	320±34	393±46	23.1	0.002
Mass fraction				
Cortical shell	0.33±0.03	0.34±0.03	2.7	0.52
Trabecular bone (1—shell mass fraction)	0.67±0.03	0.66±0.03	−1.3	0.52
Cross-sectional area (mm^2)	126±52	118±20	−6.3	0.67

Mean±SD.

[a] Percent difference calculated with respect to the control means.

[b] Difference between the control and suppressed groups, Student's t-test.

Table 2

Comparison of FE-computed load sharing and stiffness outcomes between the control- and RIS-suppressed groups.

	Control	RIS-suppressed	Percent[a]	*p*-Value[b]
Maximum load fraction				
Cortical shell	0.56±0.04	0.53±0.04	−5.0	0.17
Trabecular bone	0.81±0.03	0.78±0.04	−3.6	0.08
Trabecular-compartment stiffness (kN/mm)	10.9±1.9	13.7±2.2	26.0	0.01
Whole-vertebra stiffness (kN/mm)	17.0±2.2	20.5±3.1	20.9	0.02
Cortical shell stiffness (kN/mm)[c]	6.1±0.8	6.8±1.1	11.7	0.15
Ratio of trabecular- compartment stiffness to whole- vertebra stiffness	0.64±0.05	0.67±0.03	4.7	0.11

All stiffness (and modulus) values computed assumed the same value of tissue elastic modulus throughout (see text for details).

[a] Percent difference calculated with respect to the control means.

[b] Difference between the control and suppressed groups, student's *t*-test.

[c] Computed as the difference between the whole-vertebra stiffness and trabecular-compartment stiffness.